Protective effects of budesonide on LPS-induced podocyte injury by modulating macrophage M1/M2 polarization: Evidence from *in vitro* and *in silico* studies

XILAN ZHANG[1], GUANGYING WANG[2], DAYUE SHEN[1], YATING FENG[1], YAN ZHANG[3], CHAO ZHANG[3], YUANPING LI[2] and HUI LIAO[2]

[1]School of Pharmacy, Shanxi Medical University, Taiyuan, Shanxi 030001; Departments of [2]Pharmacy and [3]Nephrology, Fifth Hospital of Shanxi Medical University (Shanxi Provincial People's Hospital), Taiyuan, Shanxi 030012, P.R. China

Received March 31, 2022; Accepted June 21, 2022

DOI: 10.3892/etm.2022.11526

Abstract. Budesonide (Bud), one of the most widely used lung medicines, is currently used as a repurposing medicine for immunoglobulin A nephropathy (IgAN) treatment. The progression of IgAN is related to inflammation involving macrophages and podocytes. The present study aimed to explore the effects of Bud on classically activated (M1)/alternatively activated (M2) macrophage polarization and podocyte injury under lipopolysaccharide (LPS)-induced inflammatory stress *in vitro*. Anti-inflammatory bioinformation of Bud was identified based on the Gene Expression Omnibus database. RAW264.7 cells were treated with normal medium, LPS, curcumin (Cur, positive control), or Bud 5, 10, or 20 μM. The expression levels of inducible nitric oxide synthase (iNOS), TNF-α, mannose receptor (CD206) and arginase (Arg)-1 were quantified by western blotting. The collected supernatants from macrophages were termed (Nor)MS, (LPS)MS, (Cur)MS and (Bud)MS. The TNF-α, IL-1β and nitric oxide (NO) levels in the supernatants were evaluated by ELISA and Griess assay. The podocytes were cultured in different supernatants and their survival rates were assessed by bromodeoxyuridine assay. TNF signaling is an important pathway by which Bud exerts anti-inflammatory activities. Compared with the LPS group, 5, 10 and 20 μM Bud significantly increased Arg-1 and decreased iNOS expression (Six: P<0.05) and 20 μM Bud significantly increased Arg-1 and CD206 and decreased iNOS and TNF-α expression (Four: P<0.05). Cur significantly decreased iNOS and TNF-α expression (Two: P<0.05). Compared with LPS, 5, 10 and 20 μM Bud and Cur significantly decreased TNF-α, IL-1β and NO levels (All: P<0.05). The podocyte survival rates of (Bud)MS and (Cur)MS were significantly higher than those of (LPS)MS (Four: P<0.05). The protective effect of Bud on podocyte injury is related to its modulation of M1/M2 polarization.

Correspondence to: Professor Yuanping Li or Professor Hui Liao, Department of Pharmacy, Fifth Hospital of Shanxi Medical University (Shanxi Provincial People's Hospital), 29 Shuangtasi Street, Taiyuan, Shanxi 030012, P.R. China
E-mail: liyuanping1699@163.com
E-mail: huiliao@263.net

Key words: budesonide, bioinformation, macrophage polarization, podocyte injury

Introduction

For the first 40 years of the 20th century, when asthma occurred, the treatments were given by injection or oral administration of the adrenergic agonist epinephrine and the phosphodiesterase inhibitor theophylline (1). In 1930, epinephrine became available as an aerosol. To date, repurposing drugs as inhaled therapies in asthma has made progress in drug delivery to the action site. More importantly, inhaled therapies permit the prophylactic treatment of asthma. As a nonhalogenated corticosteroid, budesonide (Bud) was developed in the early 1970s and was available as an inhaled steroid by 1982 (1). It is now one of the most widely used inhaled medicines in lung diseases such as asthma and chronic obstructive pulmonary disease (COPD) worldwide (2).

As a repurposing drug, Bud showed its efficacy again in a recent double-blind, random, placebo-controlled phase 2b trial in patients with immunoglobulin A nephropathy (IgAN) (3). IgAN is the commonest type of glomerulonephritis in Asia and the western world (4). The mainstay of therapy is therefore optimized supportive care, i.e., measures that lower blood pressure, reduce proteinuria and help to decrease nonspecific insults to the kidneys (4). Glomerular podocyte injury is a key factor associated with proteinuria in IgAN (5). Clinical research shows that Bud is effective in the treatment of patients with IgAN at high risk of progression in terms of reducing proteinuria and preserving renal function over 24 months of therapy (6). However, whether Bud can reduce proteinuria by protecting podocytes *in vitro* and *in vivo* remains unclear.

Complex factors are involved in the development and progression of IgAN. Autoimmunity and inflammation are considered to be the basic mechanisms; however, the exact pathogenesis remains to be elucidated (7). To explore a possible protective effect of Bud on podocyte injury under inflammatory stress (8), the Gene Expression Omnibus (GEO) was used

in the present study to identify the induced anti-inflammatory genes in humans involved in transcription and signaling following inhalation of Bud (9). Differentially expressed genes (DEGs) were identified between the volunteers who inhaled Bud or placebo randomly (9). The results showed that, based on downregulated DEGs, the TNF signaling pathway served an important role when Bud exerted anti-inflammatory effects (The results are shown in Table I).

The authors' previous *in vitro* study suggests that increased TNF-α protein expression in polarized macrophages is related to podocyte injury (10). With lipopolysaccharide (LPS)-induced RAW264.7 macrophages, the effects of Bud on the protein expression of two markers of classically activated macrophages (M1), inducible nitric oxide synthase (iNOS) and TNF-α and two markers of alternatively activated macrophages (M2), mannose receptor (CD206) and arginase (Arg)-1, were identified (10) and the effects of Bud on LPS-induced podocyte injury by modulating M1/M2 polarization were further explored in the present study (Fig. 1).

Materials and methods

Microarray material and microarray data. GEO (http://www.ncbi.nlm.nih.gov/geo/) is an international public repository that archives and freely distributes high-throughput gene expression and other functional genomics datasets (11). A gene expression dataset, namely, GSE83233 (https://www.ncbi.nlm.nih.gov/geo/query/acc.cgi?acc=GSE83233) 'An inhaled dose of budesonide induces genes involved in transcription and signaling in human airways', was downloaded from GEO [GPL15207 platforms, (PrimeView) Affymetrix Human Gene Expression Array]. In the study (9), healthy male, nonsmoker, nonallergic volunteers (age 18-50 years) with normal lung function were recruited into this prospective, double-blind, placebo-controlled, randomized, two-period crossover study involving an initial screening visit, followed by two intervention visits. Participants were screened at visit one to fulfil the study eligibility criteria. At visit two, volunteers were randomized to receive inhaled Bud (1,600 μg) or placebo, both via Turbuhaler. Then, at two to three weeks later, at visit three, participants received either Bud or placebo, as appropriate, to complete both study arms. At 6 h after placebo or Bud inhalation, bronchial biopsies were obtained via bronchoscopy (9). The study protocol and consent form were approved by the Conjoint Health Research Ethics Board at the University of Calgary and Alberta Health Services and the ethical approval number was 23241.

Identification of DEGs. The DEGs in the Bud and placebo specimens were selected from GEO2R (http://www.ncbi.nlm.nih.gov/geo/geo2r), which is a platform for examining DEGs across experimental conditions by comparing multiple datasets in GEO series. The genes with multiple probes were averaged and the probes that lacked gene symbols were removed. The DEGs with a |logFC (fold change)| >0 and P<0.01 were screened out and represented statistical significance.

Gene Ontology (GO) and Kyoto Encyclopedia of Genes and Genomes (KEGG) enrichment analysis of DEGs. The database for annotation, visualization and integrated discovery (DAVID), which can be freely accessed (http://david.ncifcrf.gov), is a web-based online bioinformatics resource that aims to provide tools for the functional interpretation of large lists of genes and proteins (12). In addition, GO, a significant bioinformatics tool, enables the annotation of genes according to biological processes (13). The KEGG is a knowledge-based platform for the systematic analysis of gene functions, linking genomic information with higher-order functional information (14,15). The DAVID online database was used to study the functions of DEGs. P<0.05 was considered to indicate a statistically significant difference. ImageGP (http://www.ehbio.com/ImageGP/) was used to draw enrichment plots for GO and KEGG.

Cell source and culture. A mouse macrophage RAW264.7 cell line was purchased from Procell Life Science & Technology Co., Ltd. According to the instructions, the cells were maintained in RPMI-1640 medium (Beijing Solarbio Science & Technology Co., Ltd.) supplemented with 10% fetal bovine serum (FBS; Gibco; Thermo Fisher Scientific, Inc.), 100 U/ml penicillin and 100 μg/ml streptomycin (Shanxi MiniBio Technology Co., Ltd.) in a 5% CO_2 incubator at 37˚C. The medium was replaced the next day.

A conditionally immortalized mouse MPC-5 podocyte cell line was purchased from Fuheng Biology Company and cultured in RPMI-1640 medium supplemented with 10% FBS and recombinant IFN-γ (cat. no. G1021; APeXBIO Technology LLC) at 33˚C. Podocytes were reseeded and cultured in RPMI-1640 medium with 10 mg/ml type-I collagen (BD Biosciences) at 37˚C without IFN-γ for 7-15 days before testing.

Cytotoxicity of Bud and LPS on RAW264.7 and MPC-5 cells. RAW264.7 cells and MPC-5 cells were seeded into 96-well plates separately at a density of $1x10^6$ cells/ml and cultured in 10% FBS RPMI-1640 medium for 24 h at 37˚C. Following another 24 h treatment with Bud (cat. no. 200721527; Chiatai Tianqing Pharmaceutical Group Co., Ltd.) at 5, 10, 20, 40 and 80 μM (16,17), LPS at 0.02, 0.10, 0.50, 2.50 and 12.5 μg/ml at 37˚C (18-20). The supernatants were removed and each well was washed with PBS before the addition of 10% FBS RPMI-1640 medium and 10 μl CCK-8 reagent (Shanxi MiniBio Technology Co., Ltd.). Cell viability was determined by measuring the absorbance at 450 nm using a microporous plate reader (Model 550; Bio-Rad Laboratories, Inc.) after an incubation period of 2 h at 37˚C. The average optical density was determined by examining six wells per group.

Establishment of LPS-induced M1 polarization. Based on the cytotoxicity results of LPS on RAW264.7 cells. LPS (0.10 μg/ml) was used to induce macrophage polarization to the M1 subtype for 24 h at 37˚C. The nitric oxide (NO) level was tested with the Griess assay (21). Nitrite, a stable end-product of NO metabolism, was measured using the Griess reaction. Culture media of the RAW 264.7 cells (100 μl) was mixed with an equal volume of Griess reagent (Yantai Science & Biotechnology Co. Ltd.), followed by spectrophotometric measurement at 540 nm. Nitrite concentrations in the culture media were determined by comparison with a sodium nitrite standard curve. All experiments were repeated three times.

Table I. The 10 KEGG pathways based on downregulated DEGs.

Term	Description	Count in gene set	Gene ratio	P-value
hsa04668	TNF signaling pathway	10	3.257	$1.966x10^{-4}$
hsa05146	Amoebiasis	9	2.932	$9.259x10^{-4}$
hsa04670	Leukocyte transendothelial migration[a]	9	2.932	$1.573x10^{-3}$
hsa00280	Valine, leucine and isoleucine degradation	5	1.629	$1.222x10^{-2}$
hsa04068	FoxO signaling pathway[a]	8	2.606	$1.429x10^{-2}$
hsa05222	Small cell lung cancer	6	1.954	$2.330x10^{-2}$
hsa05169	Epstein-Barr virus infection	7	2.280	$2.949x10^{-2}$
hsa04152	AMPK signaling pathway	7	2.280	$3.053x10^{-2}$
hsa05200	Pathways in cancer	14	4.560	$3.785x10^{-2}$
hsa05160	Hepatitis C	7	2.280	$4.228x10^{-2}$

The 10 significant KEGG pathways were ranked according to their P-value. [a]These two are also shown in Table II. KEGG, Kyoto Encyclopedia of Genes and Genomes; DEGs, differentially expressed genes.

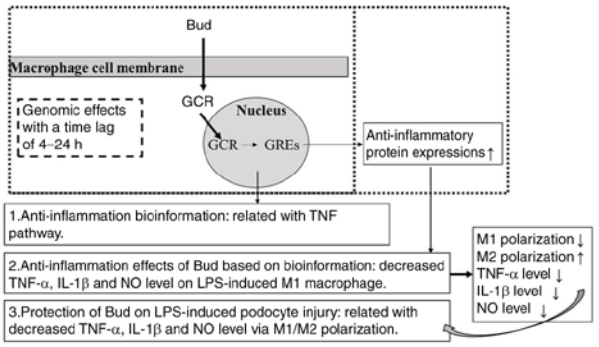

Figure 1. Protective effect of Bud on LPS-induced podocyte injury mediated via macrophage M1/M2 polarization. Bud, budesonide; GCR, glucocorticoid receptors; GREs, glucocorticoid response elements; NO, nitric oxide; LPS, lipopolysaccharide; M1, classically activated macrophages; M2, alternatively activated macrophages.

Effects of Bud on iNOS, TNF-α, Arg-1 and CD206 protein expression in M1 macrophages. The protein expression levels of iNOS, TNF-α, Arg-1 and CD206 at different concentrations of Bud (5, 10, 20 μM) in 0.10 μg/ml LPS-cultured macrophages were tested by western blotting. RPMI-1640 was used as the normal control, LPS was used as the model control and 10 μM curcumin (cat. no. C7090; Beijing Solarbio Science & Technology Co., Ltd.; purity: 95.0%) was used as the positive control (22). The treated cells ($1x10^6$ cells/ml) were removed from the culture media and lysed with RIPA lysis buffer from Beijing Solarbio Science & Technology Co., Ltd. for 30 min. The protein concentrations were determined using a BCA Protein Assay kit from Beijing Solarbio Science & Technology Co., Ltd. Samples containing 50 μg of protein were resolved by 10% SDS-PAGE electrophoresis and transferred to polyvinylidene fluoride membranes (MilliporeSigma) in a buffer tank with platinum wire electrodes. After immersing the membranes into 5% nonfat dried milk (diluted in 0.1% (v/v) Tween-20 PBS) for 2 h at room temperature to block nonspecific binding, the membranes were incubated overnight with a primary antibody against iNOS at a 1:2,000 dilution (cat. no. 18985-1-AP; ProteinTech Group, Inc.), a primary antibody against TNF-α (cat. no. bs-2081R; Bioss) at a 1:1,000 dilution, a primary antibody against CD206 (cat. no. bs-21473R; Bioss) at a 1:1,000 dilution and a primary antibody against Arg-1 (cat. no. 16001-1-AP; ProteinTech Group, Inc.) at a 1:5,000 dilution at 4˚C. The membranes were then washed three times (10 min each) and incubated with the corresponding secondary IgG conjugated to HRP antibody (cat. no. SA00001-2; ProteinTech Group, Inc.) at room temperature for 1 h. The results were finally analyzed by the Quantity One analysis system (Bio-Rad Laboratories, Inc.). GAPDH at a dilution of 1:5,000 (cat. no. 10494-1-AP; ProteinTech Group, Inc.) was used as the internal loading control.

Effects of Bud on TNF-α, IL-1β and NO levels in M1 macrophages. RAW264.7 cells ($1x10^6$ cells/ml) were treated with 0.10 μg/ml LPS for 2 h and then treated with Bud (5, 10, 20 μM) in LPS-cultured macrophages for another 22 h at 37˚C. RPMI-1640 was designated the normal control for all the above-tested groups and the curcumin group was designated the positive control (22). Cell supernatants were then harvested and centrifuged at 1,500 x g for 10 min at 4˚C. TNF-α levels were determined using an ELISA kit (cat. no. MM-0132M1; Jiangsu Meimian Industrial Co., Ltd.). IL-1β levels were tested with an ELISA kit (cat. no. MM-0040M1; Jiangsu Meimian Industrial Co., Ltd.). The absorbance was measured using a microplate reader. Each sample underwent repeated testing four times.

The NO levels of the normal control, curcumin control and Bud at 5, 10 and 20 μM were also tested with the Griess assay (21). All experiments were repeated three times.

Collection of the supernatant from macrophages (23). RAW264.7 cells were seeded into six-well plates and cultured in normal control, LPS model and curcumin positive, Bud 5, 10, 20 μM at 37˚C, respectively. The supernatants were collected 24 h later, centrifuged at 1,500 x g for 15 min at 4˚C and labeled as (Nor)MS, (LPS)MS, (Cur)MS, (Bud5)MS, (Bud10)MS and (Bud20)MS. The collected supernatants were centrifuged for the second time at 1,500 x g for 10 min at 4˚C, filtered with a 0.22 μm sterile membrane and stored at -80˚C for further use.

Determination of LPS-induced podocyte injury (24). Podocytes ($5x10^5$ cells/ml) were cultured with normal medium, 0.1 μg/ml LPS, 10 μM curcumin, 5 μM Bud, 10 μM Bud, or 20 μM Bud and (Nor)MS, (LPS)MS, (Cur)MS, (Bud5)MS, (Bud10)MS, or (Bud20)MS for 22 h at 37˚C. Podocytes were then seeded into 96-well plates. The cells were subsequently treated with bromodeoxyuridine (BrdU) reagent during the final 2 h of incubation. The BrdU cell proliferation assay kit (cat. no. 2750; MilliporeSigma) was performed according to the manufacturer's protocol. The survival rate of the normal group was 100% and the survival rate of cells in the other groups was compared with that of the normal group. The mean was obtained by examining six wells per group.

Statistical analysis. SPSS 19.0 software (IBM Corp.) was used for statistical analysis. All the data were expressed as the mean ± standard deviation (SD) of the mean. A two independent sample unpaired Student's t-test was used to analyze differences between two groups. One-way analysis of variance with Bonferroni's posttest was used when more than two groups were present. P<0.05 was considered to indicate a statistically significant difference.

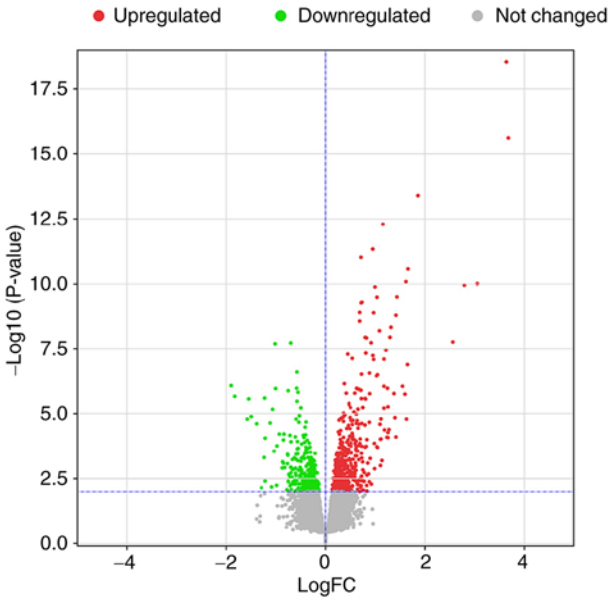

Figure 2. All DEGs between the budesonide group and placebo group in the human airway. A significant DEG was selected with a |logFC (fold change)| >0 and P<0.01 among the mRNA expression profiling set GSE83233. DEG, differentially expressed gene.

Results

DEGs results. After standardization of the microarray data, all DEGs between the Bud group and placebo group in GSE83233 were identified, as shown in Fig. 2. The dataset consisted of a total of 832 significant DEGs [|logFC (fold change)| >0 and P<0.01], of which 311 DEGs were downregulated and 521 were upregulated.

GO and KEGG results. Functional and pathway enrichment analyses were conducted on DEGs for further analyses of biological classification. Based on total DEGs, the numbers of significant cell component (CC), molecular function (MF), biological process (BP) and KEGG pathways were 22, 34, 142 and 37, respectively (P<0.05). The top 20 CC, MF, BP and KEGG terms are shown separately in Fig. 3. The results indicated that the main CC terms included the nucleus, cytoplasm and plasma membrane. The MF terms were mainly related to protein binding, transcription factor activity, sequence-specific DNA binding, etc. The main BP terms included positive/negative regulation of transcription from RNA polymerase II promoter and positive/negative regulation of transcription, DNA-templated and inflammatory response. KEGG results showed that a number of pathways were involved in the inflammatory response, such as the forkhead box subgroup O (FoxO) signaling pathway and the TNF signaling pathway.

Based on upregulated DEGs, there were 18 significant KEGG items (P<0.05) among the 31 items in Table II. The FoxO signaling pathway had the lowest P-value and the second highest gene ratio in KEGG. Based on downregulated DEGs, further KEGG study showed that there was a total of 16 items in which the 10 had significant differences (P<0.05) in Table I. The TNF signaling pathway had the lowest P-value and the second highest gene ratio.

Cytotoxicity results of Bud and LPS. Fig. 4A shows that Bud inhibited the growth of RAW 264.7 cells in the range of 40-80 μM (cell viability at 40 μM: 90.5±4.5 and 80 μM: 83.8±8.0%) and had significant differences compared with 0 μM Bud (100.3±4.0%; P=0.009 and P=0.006). Fig. 4A also shows that the viability of MPC-5 cells treated with 80 μM Bud was (86.3±7.5)%, which was significantly different from that of cells treated with 0 μM Bud (101.4±9.7%; P=0.005). The above results suggested that Bud at 5, 10 and 20 μM could be used to test its effects on macrophage polarization and podocyte injury.

Fig. 4B shows that LPS inhibited the growth of RAW 264.7 cells at 2.50 μg/ml and 12.5 μg/ml (cell viability: 91.1±4.0 and 85.1±7.2%) and had a significant difference compared with 0 μg/ml LPS (P=0.010 and P=0.008). According to the above results, LPS at 0.02, 0.10 and 0.50 μg/ml could be used on RAW 264.7 cells to induce M1 polarization.

The cell survival rates of MPC-5 cells treated with different concentrations of LPS are shown in Fig. 4B. The results showed that compared with 0 μg/ml LPS, LPS had significant cytotoxicity on MPC-5 cells at 0.10, 0.50 μg/ml, 2.50 and 12.5 μg/ml (four: P<0.01). In this case, 0.10, 0.50, 2.50 and 12.5 μg/ml LPS could be used on MPC-5 cells to establish a podocyte injury model.

Establishment of LPS-induced M1 polarization. Compared with NO production in 0 μg/ml LPS (normal control; 3.3±0.3 μM), NO production significantly increased after macrophages were cultured with 0.10 μg/ml LPS for 24 h (77.6±1.5 μM; P<0.001).

When Bud was added to RAW264.7 cells and cultured for 24 h separately, the results showed that 5, 10 and 20 μM Bud had no significant effects on NO production compared with the normal control (4.0±0.1, 4.5±0.6, 4.0±0.2 μM; three: P=NS). Additionally, compared with the normal control, curcumin did not increase NO production significantly (4.3±0.2 μM; P=NS).

Table II. The 18 KEGG pathways based on upregulated DEGs.

Term	Description	Count in gene set	Gene ratio	P-value
hsa04068	FoxO signaling pathway[a]	16	3.101	1.948×10^{-5}
hsa04960	Aldosterone-regulated sodium reabsorption	8	1.550	1.888×10^{-4}
hsa04060	Cytokine-cytokine receptor interaction	19	3.682	6.581×10^{-4}
hsa04722	Neurotrophin signaling pathway	11	2.132	4.605×10^{-3}
hsa04062	Chemokine signaling pathway	14	2.713	6.059×10^{-3}
hsa05100	Bacterial invasion of epithelial cells	8	1.550	1.145×10^{-2}
hsa00760	Nicotinate and nicotinamide metabolism	5	0.969	1.251×10^{-2}
hsa04710	Circadian rhythm	5	0.969	1.578×10^{-2}
hsa05202	Transcriptional misregulation in cancer	12	2.326	1.677×10^{-2}
hsa04064	NF-kappa B signaling pathway	8	1.550	1.997×10^{-2}
hsa04662	B cell receptor signaling pathway	7	1.357	2.156×10^{-2}
hsa04670	Leukocyte transendothelial migration[a]	9	1.744	2.916×10^{-2}
hsa04910	Insulin signaling pathway	10	1.938	3.079×10^{-2}
hsa04923	Regulation of lipolysis in adipocytes	6	1.163	3.150×10^{-2}
hsa04015	Rap1 signaling pathway	13	2.519	3.476×10^{-2}
hsa04630	Jak-STAT signaling pathway	10	1.938	4.038×10^{-2}
hsa04360	Axon guidance	9	1.744	4.809×10^{-2}
hsa04666	Fc gamma R-mediated phagocytosis	7	1.357	4.971×10^{-2}

The 18 significant KEGG pathways were ranked according to their P-value. [a]These 2 items are also shown in Table I. KEGG, Kyoto Encyclopedia of Genes and Genomes; DEGs, differentially expressed genes.

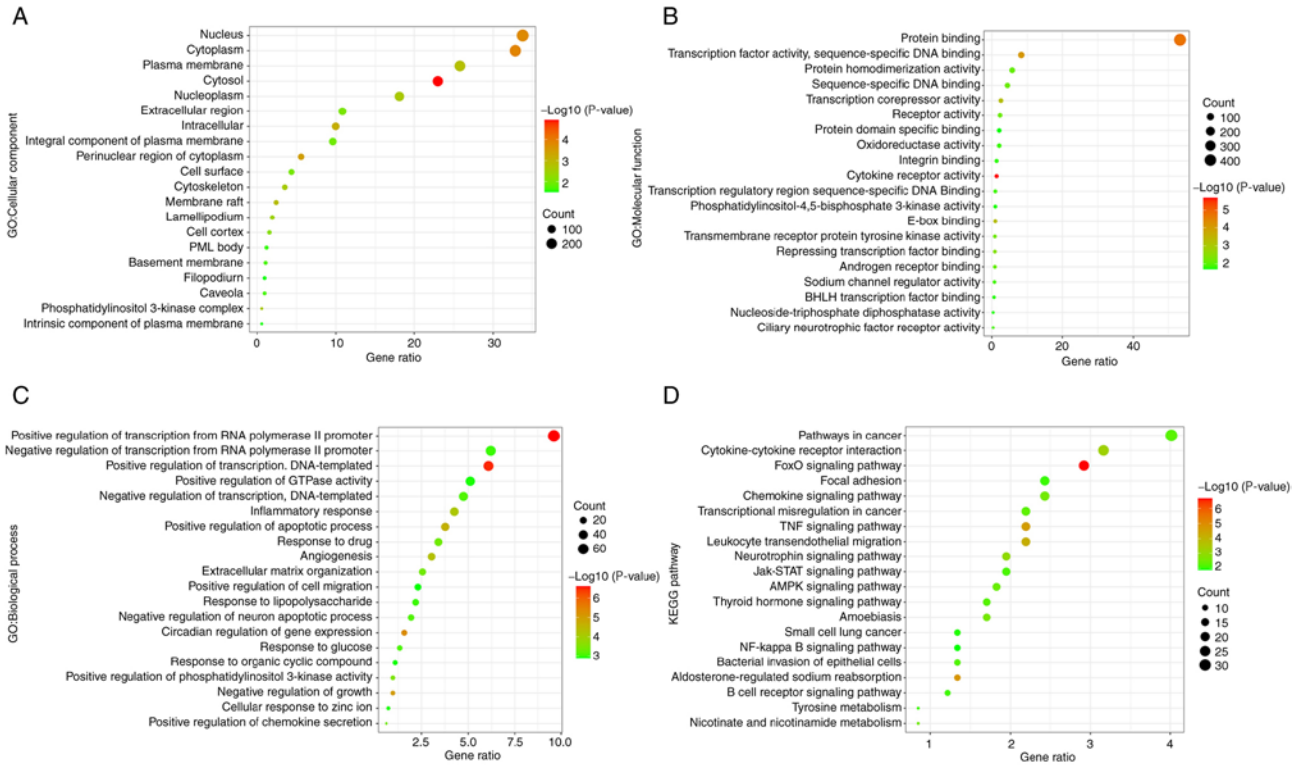

Figure 3. GO and KEGG analysis. The top 20 items in (A) CC, (B) MF and (C) BP. (D) The top 20 items in KEGG are all ranked according to their P-value. Based on total DEGs, the total numbers of significant CC, MF, BP and KEGG pathway were 22, 34, 142 and 37, respectively ($P<0.05$). GO, Gene Ontology; KEGG, Kyoto Encyclopedia of Genes and Genomes; CC, cell component; MF, molecular function; BP, biological processes.

Effects of Bud on iNOS, TNF-α, Arg-1 and CD206 protein expression in M1 macrophages. Fig. 5A and B shows the CD206, Arg-1, TNF-α and iNOS protein bands of the normal, LPS model, curcumin and Bud at three different concentrations.

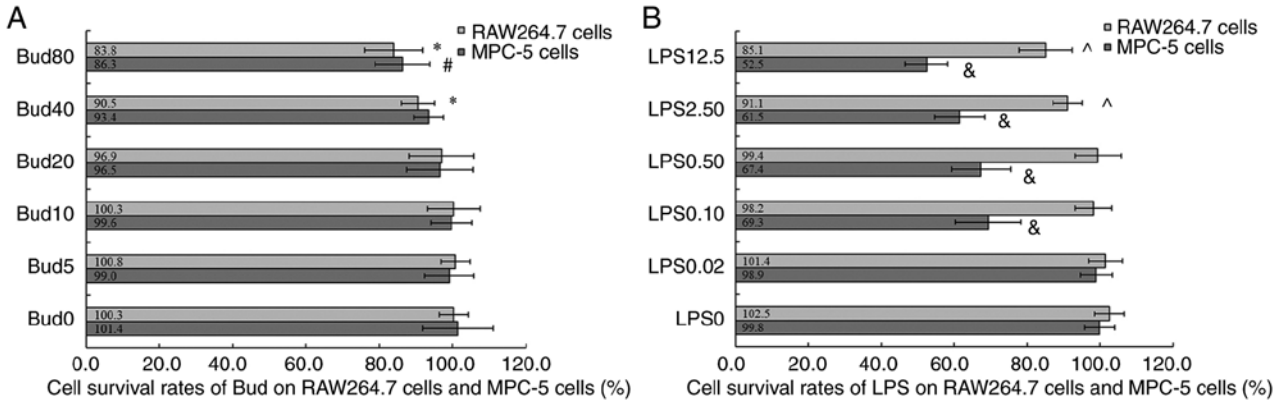

Figure 4. Cytotoxicity of Bud and LPS on RAW264.7 macrophage cells and MPC-5 podocyte cells. (A) Bud. (B) LPS. Values are expressed as the mean ± SD (n=6). *P<0.05, vs. Bud0 in RAW264.7 cells. #P<0.05, vs. Bud0 in MPC-5 cells. ^P<0.05, vs. LPS0 in RAW264.7 cells. &P<0.05, vs. LPS0 in MPC-5 cells. Bud, budesonide; LPS, lipopolysaccharide; Bud0, Bud 0 μM; Bud5, Bud 5 μM; Bud10, Bud 10 μM; Bud20, Bud 20 μM; Bud40, Bud 40 μM; Bud80, Bud 80 μM; LPS0, lipopolysaccharide 0 μg/ml; LPS0.02, lipopolysaccharide 0.02 μg/ml; LPS0.10, lipopolysaccharide 0.10 μg/ml; LPS0.50, lipopolysaccharide 0.50 μg/ml; LPS2.50, lipopolysaccharide 2.50 μg/ml; LPS12.5, lipopolysaccharide 12.5 μg/ml.

Compared with the normal control, LPS significantly increased TNF-α and iNOS protein expression (P=0.025; P=0.025) while decreasing Arg-1 and CD206 protein expression (CD206: P<0.001). As the positive control, curcumin significantly decreased TNF-α and iNOS protein expression compared with the LPS model (P=0.004; P=0.013). The above results are shown in Fig. 5.

The results also showed the effects of 5, 10 and 20 μM Bud on CD206, Arg-1, TNF-α and iNOS protein expression, as shown in Fig. 5C-F. Compared with the LPS model, 5 μM Bud significantly increased Arg-1 and CD206 expression (P<0.001; P=0.002) and decreased iNOS expression (P=0.021) and 10 μM Bud significantly increased Arg-1 expression (P=0.030) and decreased TNF-α and iNOS expression (P=0.024; P=0.002). Among the three concentrations, Bud at 20 μM not only showed a significant effect on the above four protein expression levels when compared with the LPS model (CD206: P<0.001, Arg-1: P<0.001, TNF-α: P<0.001 and iNOS: P=0.004) but also showed significantly improved effects on CD206, TNF-α and iNOS than the other two concentrations (all: P<0.05).

Effects of Bud on TNF-α, IL-1β and NO levels in M1 macrophages. The 0.10 μg/ml LPS significantly stimulated TNF-α levels (677.5±23.5 pg/ml vs. 530.8±27.0 pg/ml; P=0.003), IL-1β levels (188.8±14.6 pg/ml vs. 89.4±6.7 pg/ml; P<0.001) and NO production (77.6±1.5 μM vs. 3.3±0.3 μM; P<0.001) compared with the normal group. When compared with the LPS group, the positive curcumin significantly decreased the TNF-α level to (627.2±23.3 pg/ml; P=0.039), significantly decreased the IL-1β level to (122.6±6.0 pg/ml; P=0.006) and significantly decreased NO production to (51.2±1.0 μM; P<0.001).

Compared with the LPS group, Bud at 5, 10 and 20 μM all showed significant decreasing effects on IL-1β levels and NO production (six: P<0.05). The decreasing effects of Bud on NO production occurred in a significant dose-dependent manner (40.8±1.2 μM NO production at 5 μM vs. 35.4±0.7 μM NO production at 10 μM vs. 8.8±0.3 μM NO production at 20 μM; three: P<0.05). Additionally, compared with the LPS group, Bud at 10 and 20 μM showed significant effects on decreasing TNF-α levels (P=0.026; P<0.001).

Bud at 20 μM showed a significantly improved decreasing effect on NO production and TNF-α levels than curcumin (P<0.001 and P=0.001), but Bud at 20 μM and curcumin did not show a significant difference in decreasing IL-1β levels (P=NS). All of the above results are shown in Fig. 6.

The results of Bud on LPS-induced podocyte injury. Fig. 7 shows that the MPC-5 cell survival rates between normal control and LPS model were significantly different (P<0.001). Compared with LPS, (LPS)MS further decreased the cell survival rate significantly (54.6±5.2% vs. 66.1±7.5%; P=0.001).

Additionally, compared with LPS, curcumin significantly increased the cell survival rate (84.1±5.0%; P=0.003), but Bud at 5, 10 and 20 μM did not show any significant influence on the cell survival rate under LPS stress (three: P=NS).

Compared with (LPS)MS, (Cur)MS (80.6±4.9%; P=0.001) and (Bud5)MS (66.0±5.0%; P=0.027), (Bud10)MS (74.0±4.5%; P=0.002), (Bud20)MS (79.8±5.8%; P=0.001) all showed significantly increased effects on cell survival rates. The increasing effect on the cell survival rate of (Bud20)MS was significantly improved compared with that of (Bud10)MS and (Bud5)MS (P=0.046; P=0.004), but there was no significant difference compared with that of (Cur)MS (P=NS).

Discussion

Glucocorticoids, including Bud, exert their activities by two main mechanisms of action: the classic genomic effects with a time lag of 4-24 h (25) and secondary nongenomic effects with a rapid action (25,26). The genomic effects develop in the cytoplasm and Bud binds to a specific receptor, forming a complex that enters the nucleus. This complex binds to specific glucocorticoid response elements in genes and increases the expression of anti-inflammatory proteins (25).

Based on the above pharmacological activities in Fig. 1, the bioinformation results in Fig. 3 could be understood easily: The highly regulated gene ratios in the nucleus, cytoplasm, plasma membrane and nucleoplasm in CC and the main

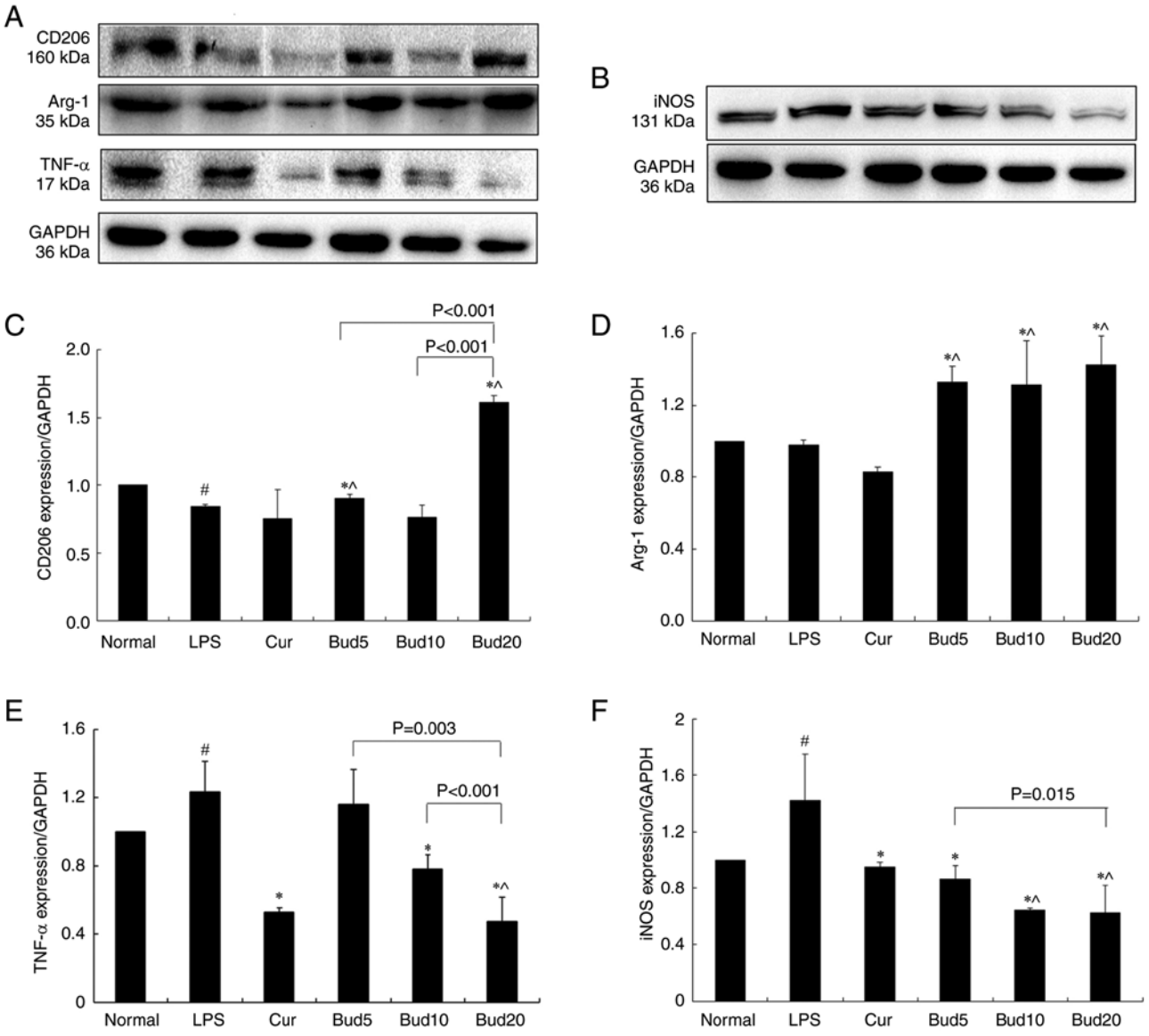

Figure 5. Effects of Bud on CD206, Arg-1, TNF-α and iNOS protein expression in LPS-induced RAW264.7 cells. (A) CD206, Arg-1 and TNF-α protein expression. (B) iNOS protein expression. The results of CD206, Arg-1, TNF-α and iNOS are represented in (C), (D), (E) and (F), respectively. All results were expressed as a ratio with respect to the control and represented as the mean ± SD (n=3). #P<0.05, LPS vs. normal. *P<0.05, Cur and Bud vs. LPS. ^P<0.05, Bud vs. normal. Bud, budesonide; CD206, mannose receptor; Arg-1, arginase-1; iNOS, inducible nitric oxide synthase; LPS, lipopolysaccharide; Bud5, Bud 5 μM; Bud10, Bud 10 μM; Bud20, Bud 20 μM; Cur, curcumin.

regulated MFs include protein binding, transcription factor activity, sequence-specific DNA binding, protein homodimerization activity and receptor activity.

In vitro research shows that transcriptomic changes in response to glucocorticoid exposure are similar in airway smooth muscle derived from donors with fatal asthma and donors without asthma, with enriched ontological pathways that included cytokine- and chemokine-related categories (27). A clinical study shows that an inhaled dose of Bud induced genes involved in transcription to enhance anti- and proinflammatory effector genes (9). With GSE83233 information, the present study confirmed the relationships among the positive/negative regulation of transcription from RNA/DNA and the inflammatory response in BP results.

As an anti-inflammatory agent, Bud participates in a number of inflammatory pathways, such as NF-κB signaling in cigarette smoke-induced airway inflammation rats (28), FoxO and PI3K-Akt signaling in primary human bronchial epithelial cells and the TNF signaling pathway (29). All these inflammatory signals are shown in Fig. 3D. The present study indicates that the TNF signaling pathway is important for the anti-inflammatory effects of Bud.

Clinically, montelukast sodium plus inhaled Bud has efficacy in pediatric asthma (30), in children with cough variant asthma (31) and in elderly patients with asthma (32). All these efficacies are related to the effects of Bud on decreasing TNF-α levels (30-32). Animal research shows that Bud markedly attenuates pathological injury in mice with acute lung injury (ALI) and reduced TNF-α and IL-1β levels in the bronchoalveolar lavage fluid (BALF) and serum of mice with ALI. Additionally, Bud obviously reduced the numbers of macrophages in the BALF of mice with ALI (33).

Macrophages are the most abundant immune cells in the lung (~70% of all immune cells) and they serve important

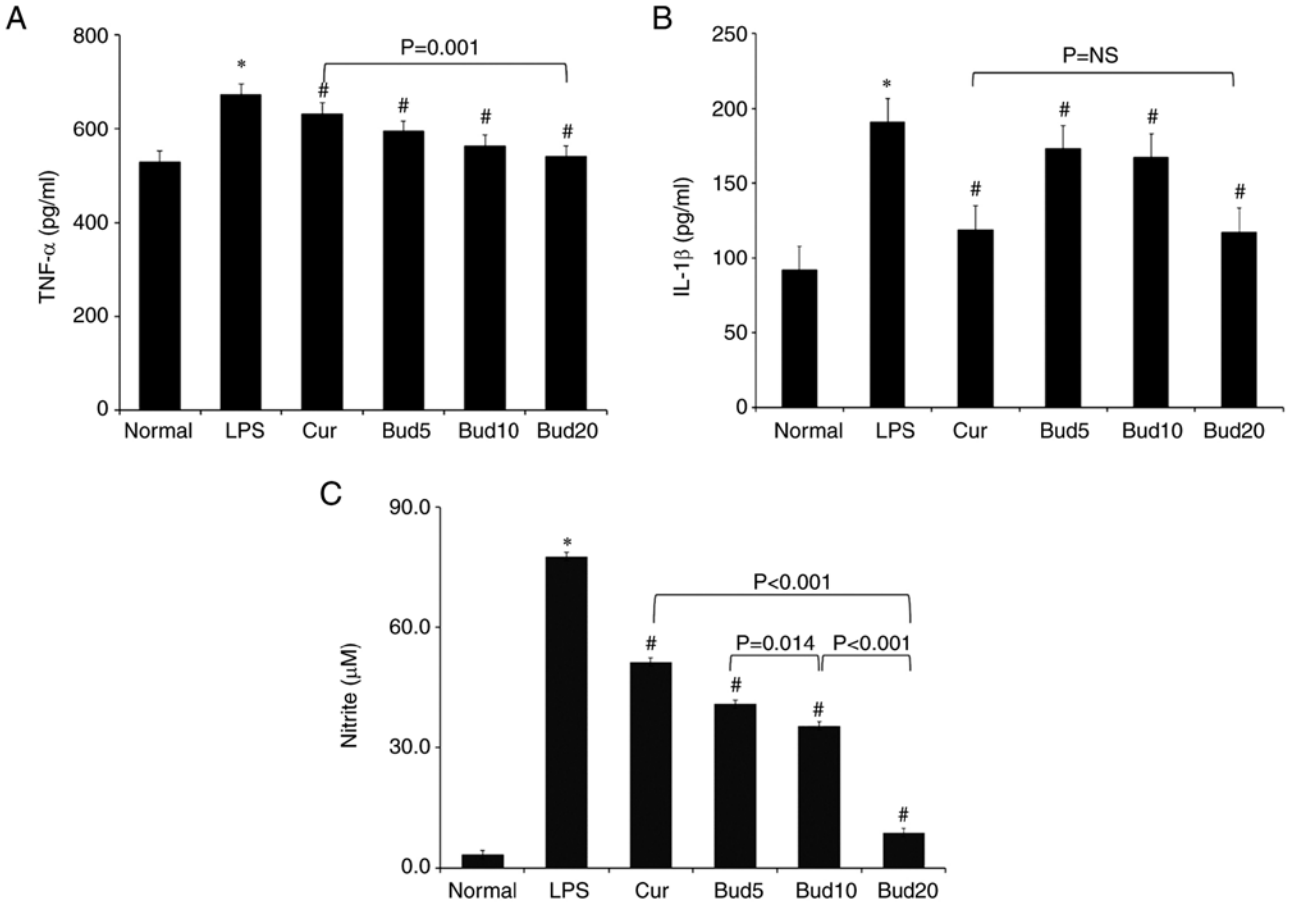

Figure 6. Effects of Bud on TNF-α and IL-1β levels and nitric oxide production in RAW 264.7 cells. (A) TNF-α level. (B) IL-1β level and (C) Nitric oxide production. Values of TNF-α and IL-1β are expressed as the mean ± SD (n=4). Values of nitric oxide production were expressed as the mean ± SD in triplicates. *P<0.05, vs. normal. #P<0.05, vs. LPS. LPS, lipopolysaccharide; Bud, budesonide; Bud5, Bud 5 μM; Bud10, Bud 10 μM; Bud20, Bud 20 μM; Cur, curcumin.

roles in environmental allergen-induced airway inflammation in asthma. Activated macrophages commonly exist in two distinct subtypes: the protective roles of M2 macrophages and pathogenic roles of M1 macrophages have been discussed in a number of lung diseases, including asthma and COPD (34,35). Macrophage polarization to the M1 subtype is an important specifying feature of inflammation, which is involved in the progression of pulmonary inflammation and secretion of TNF-α (36).

To date, some research on airway inflammation, M1/M2 macrophage polarization and secretion of TNF-α have been reported in asthmatic and COPD animal models and *in vitro* (37-39). Some *in vitro* M1/M2 research is also performed in human primary monocyte-derived macrophages (40) and RAW264.7 cells (35,41). According to the current *in vivo* and *in vitro* M1/M2 research in lung diseases, iNOS (36) and TNF-α (36,39,40) are important indicators of the M1 subtype and Arg-1 (36) and CD206 (35,36) are indicators of the M2 subtype.

The present study confirmed that the increased anti-inflammatory protein expression of Bud in LPS-induced macrophages was related to its regulatory effects on M1/M2 polarization. To the best of the authors' knowledge, the present study is the first to explore the effects of Bud on Arg-1 and CD206 protein expression. Bud further decreased TNF-α, IL-1β and NO levels via M1/M2 polarization.

As aforementioned, podocyte injury is a key factor associated with proteinuria in IgAN (5), in which inflammation-induced podocyte injury serves an important role (42). To establish an *in vitro* podocyte injury model, the specific LPS concentration able to induce podocyte injury was determined with a CCK-8 assay before sampling and testing. According to studies, podocyte injury can be induced by LPS at concentrations ranging from 0.1 to 10 μg/ml and the survival rate of MPC-5 ranges from 25 to 50% (18-20). As a positive control in the present study, curcumin showed significant protection against 0.1 μg/ml LPS-induced podocyte injury.

Curcumin has been reported to directly protect against podocyte injury *in vitro* and *in vivo*. The podocyte-protective effect of curcumin and its effects on the NF-κB pathway has been confirmed in a doxorubicin-induced conditionally immortalized mouse podocyte cell line (43). In another *in vitro* model, curcumin reverses angiotensin II-induced podocyte injury in a dose-dependent manner (44). Curcumin inhibits podocyte cell apoptosis and accelerates cell autophagy in diabetic nephropathy by regulating Beclin1/UVRAG/Bcl2 (45). Unlike curcumin, Bud had no direct protective effect on podocyte injury induced by LPS according to the BrdU assay.

The CCK-8 assay has been used to determine the proliferation of podocyte cells, including the MPC-5 cell line (46) and human podocytes (47). BrdU is a nucleoside analog of thymidine and its incorporation into DNA during replication

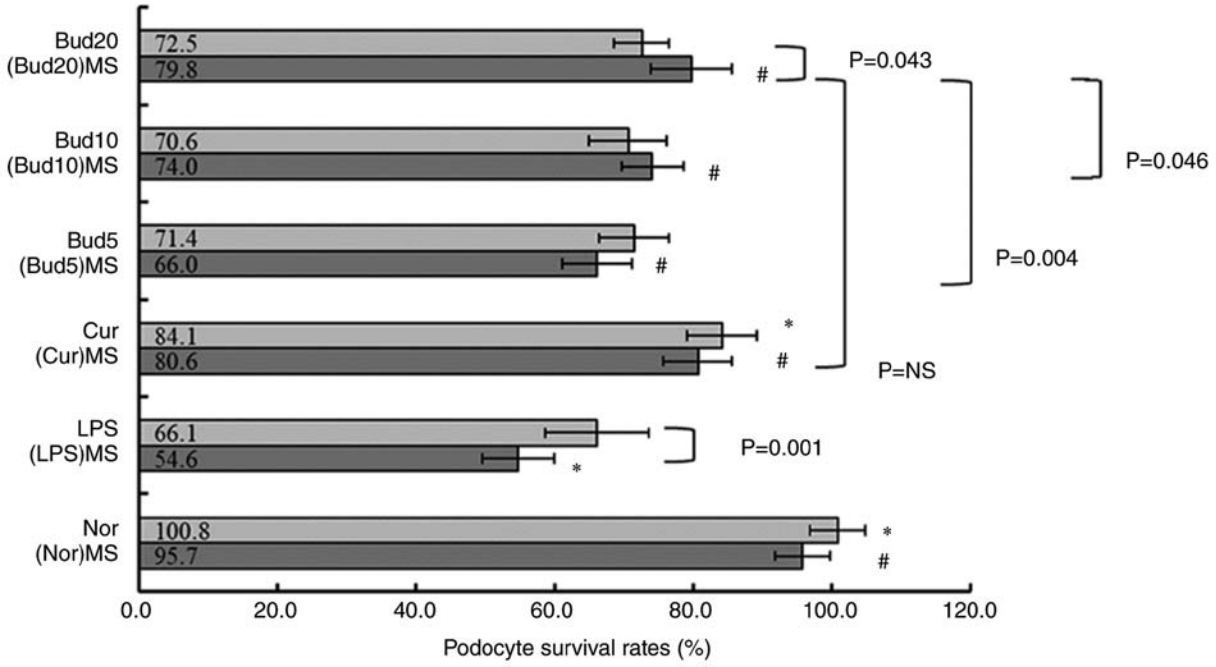

Figure 7. Cell survival rates of LPS-treated and macrophage supernatant-treated podocytes treated with Bud. Values are expressed as the mean ± SD of the mean (n=6). *P<0.05, vs. LPS. #P<0.05, vs. LPS(MS). LPS, lipopolysaccharide; Bud, budesonide; Nor, normal control; (Nor)MS, supernatants from normal-cultured macrophages; (LPS)MS, supernatants from LPS-cultured macrophages; Cur, curcumin, positive control; (Cur)MS, supernatants from Cur 10 μM and LPS-cultured macrophages; Bud5, Bud 5 μM; (Bud5)MS, supernatants from Bud 5 μM and LPS-cultured macrophages; Bud10, Bud 10 μM; (Bud10)MS, supernatants from Bud 10 μM and LPS-cultured macrophages; Bud20, Bud 20 μM; (Bud20)MS, supernatants from Bud 20 μM and LPS-cultured macrophages.

within S-phase of the cell cycle is used to quantify cell proliferation (48). In rats administered BrdU to detect cellular proliferation in kidney injury, immunohistochemical analysis indicates that the number of BrdU-positive cells is increased following kidney injury (49). In the study of NG2-lineage cells transdifferentiation following podocyte depletion, the BrdU assay has also used to detect cell proliferation (50). The GO functional enrichment analysis in the present study showed that positive/negative regulation of transcription of DNA-templated were highly enriched in BP. Nucleus and nucleoplasm were highly enriched in CC and sequence-specific DNA binding was highly enriched in MF.

A recent identification of the miRNA-mRNA network and immune-related gene signatures in IgAN by integrated bioinformatics analysis shows that infiltrating immune cells may serve significant roles in IgAN pathogenesis and that the numbers of activated macrophages increase in IgAN (51). It is reported that renal NOD-like receptor, pyrin domain-containing 3 (NLRP3) inflammasome expression is significantly increased in IgAN patients compared with normal control tissues (52). Dys-glycosylated IgA1 isolated from IgAN patient serum can induce NLRP3 expression in podocytes and initiate the interaction between podocytes and macrophage differentiation (52).

A series of cell experiments in the coculture of macrophages and podocytes (23) or isolated culture (53) examine their interaction. The present study showed that (LPS)MS, the isolated culture of LPS-treated macrophages, induced podocyte injury. Additionally, podocyte injury was more severe in (LPS)MS than in LPS.

A mechanistic study demonstrated that Tim-3 aggravates podocyte injury by promoting macrophage activation via the TNF-α pathway (54). Apart from TNF-α, a number of inflammatory factors, including IL-1β (55) and NO (53), take part in the inflammatory process and contribute to podocyte injury via macrophage polarization. The present study confirmed that Bud and curcumin indirectly protected against podocyte injury by modulating M1/M2 polarization via a reduction in TNF-α, NO and IL-1β levels. Since a number of gene expression changes occur in human airways following Bud inhalation, the above effects observed *in vitro* may be relevant to IgAN treatment of Bud (29).

Based on the foregoing, there may be a connection between the protection of Bud in podocyte injury and the regulation of Bud on macrophage polarization via the decreased TNF-α, NO and IL-1β levels.

As an inflammatory cytokine, TNF-α triggers the expression of not only inflammatory molecules but also cell adhesion molecules, including vascular cell adhesion molecule-1 (VCAM-1) (56). VCAM-1 helps regulate inflammation-associated vascular adhesion and the transendothelial migration of leukocytes, such as macrophages and T cells (56). Chronic epithelial immune activation leads to structural changes in the airways. These structural changes are driven by cell-autonomous JNK signaling and the activity of its downstream-acting transcription factor FoxO (57). This may explain the simultaneous leukocyte transendothelial migration and FoxO signaling pathway presented in Tables I and II.

Long-term use of glucocorticoids in patients will increase the risk of bone fractures (58). The FoxO signaling pathway might be associated with the adverse effects of osteoporosis (59,60). The FoxO family (FoxOs), including FoxO1,

FoxO3 and FoxO4, serve important roles in a number of diseases, such as osteoporosis and osteoarthritis. Research supports the contention that FoxOs contribute to the deleterious effects of reactive oxygen species on the skeleton (59). Inhibiting the transcription of FoxO activated by oxidative stress through antioxidative stress and positively regulating the Wnt signaling pathway can improve the osteogenic differentiation and bone formation of bone tissue (60). It might be useful to further explore the influence of Bud on FoxOs: which one takes part in anti-inflammatory action and which one causes side effects.

Bud has been one of the most widely used lung medicines worldwide for a number of years (2). Other than being used to treat the indications it was originally approved for in clinics, Bud has provided possibilities for IgAN treatment in recent years (61). IgAN is the most common type of glomerulonephritis in the world (62). IgAN patients will develop proteinuria, which will continue to worsen. Podocyte injury under inflammatory stress is a key factor associated with proteinuria in IgAN patients (5). Based on a microarray dataset GSE83233, the TNF-α pathway was identified as an important signal when Bud exerts its anti-inflammatory effects. With an *in vitro* LPS-induced podocyte injury model, the present study showed that the protective effect of Bud on podocyte injury under inflammatory stress was related to its modulation of macrophage polarization. An *in vivo* study of Bud on renal injury of IgAN should be conducted in future research.

Acknowledgements

Not applicable.

Funding

The present study was supported by Beijing Bethune Charitable Foundation (grant no. SCZ425FN) and Wu Jieping Medical Foundation (grant no. 320.6750.2021-08-11). The funders had no role in study design, data collection and analysis, decision to publish, or preparation of the manuscript.

Availability of data and materials

The *in silico* datasets generated and/or analyzed during the current study are available in the GEO repository, https://www.ncbi.nlm.nih.gov/geo/query/acc.cgi?acc=GSE83233. The *in vitro* datasets used and/or analyzed during the current study are available from the corresponding author on reasonable request.

Authors' contributions

HL and YL designed the study and drafted the manuscript. XZ performed the experiments and prepared the manuscript. GW analyzed and interpreted the data. DS, YF and CZ analyzed the data. YZ performed the statistical analysis. HL and YL confirmed the authenticity of all the raw data. All authors read and approved the final manuscript.

Ethics approval and consent to participate

Not applicable.

Patient consent for publication

Not applicable.

Competing interests

The authors declare that they have no competing interests.

References

1. Anderson SD: Repurposing drugs as inhaled therapies in asthma. Adv Drug Deliv Rev 133: 19-33, 2018.
2. Tashkin DP, Lipworth B and Brattsand R: Benefit: Risk profile of budesonide in obstructive airways disease. Drugs 79: 1757-1775, 2019.
3. Fellström BC, Barratt J, Cook H, Coppo R, Feehally J, de Fijter JW, Floege J, Hetzel G, Jardine AG, Locatelli F, *et al*: Targeted-release budesonide versus placebo in patients with IgA nephropathy (NEFIGAN): A double-blind, randomised, placebo-controlled phase 2b trial. Lancet 389: 2117-2127, 2017.
4. Floege J, Rauen T and Tang SCW: Current treatment of IgA nephropathy. Semin Immunopathol 43: 717-728, 2021.
5. Chang M, Yang B, Li L, Si Y, Zhao M, Hao W, Zhao J and Zhang Y: Modified huangqi chifeng decoction attenuates proteinuria by reducing podocyte injury in a rat model of immunoglobulin a nephropathy. Front Pharmacol 12: 714584, 2021.
6. Ismail G, Obrişcă B, Jurubiţă R, Andronesi A, Sorohan B, Vornicu A, Sinescu I and Hârza M: Budesonide versus systemic corticosteroids in IgA Nephropathy: A retrospective, propensity-matched comparison. Medicine (Baltimore) 99: e21000, 2020.
7. Wang S, Dong L, Pei G, Jiang Z, Qin A, Tan J, Tang Y and Qin W: High neutrophil-to-lymphocyte ratio is an independent risk factor for end stage renal diseases in IgA nephropathy. Front Immunol 12: 700224, 2021.
8. Wakashin H, Heymann J, Roshanravan H, Daneshpajouhnejad P, Rosenberg A, Shin MK, Hoek M and Kopp JB: APOL1 renal risk variants exacerbate podocyte injury by increasing inflammatory stress. BMC Nephrol 21: 371, 2020.
9. Leigh R, Mostafa MM, King EM, Rider CF, Shah S, Dumonceaux C, Traves SL, McWhae A, Kolisnik T, Kooi C, *et al*: An inhaled dose of budesonide induces genes involved in transcription and signaling in the human airways: Enhancement of anti- and proinflammatory effector genes. Pharmacol Res Perspect 4: e00243, 2016.
10. Li Y, Zheng D, Shen D, Zhang X, Zhao X and Liao H: Protective effects of two safflower derived compounds, kaempferol and hydroxysafflor yellow A, on hyperglycaemic stress-induced podocyte apoptosis via modulating of macrophage M1/M2 polarization. Immunol Res 2020: 2462039, 2020.
11. Al-Natour B, Rankin R, McKenna R, McMillan H, Zhang SD, About I, Khan AA, Galicia JC, Lundy FT and El-Karim IA: Identification and validation of novel biomarkers and therapeutics for pulpitis using connectivity mapping. Int Endod J 54: 1571-1580, 2021.
12. Sherman BT, Hao M, Qiu J, Jiao X, Baseler MW, Lane HC, Imamichi T and Chang W: DAVID: A web server for functional enrichment analysis and functional annotation of gene lists (2021 update). Nucleic Acids Res 50: W216-W221, 2022.
13. The Gene Ontology Consortium: The gene ontology resource: 20 years and still GOing strong. Nucleic Acids Res 47(D1): D330-D338, 2019.
14. Deng X, Gao J and Zhao F: Identification of differentially expressed genes and pathways in kidney of ANCA-associated vasculitis by integrated bioinformatics analysis. Ren Fail 44: 204-216, 2022.
15. Kanehisa M, Sato Y, Furumichi M, Morishima K and Tanabe M: New approach for understanding genome variations in KEGG. Nucleic Acids Res 47: D590-D595, 2019.
16. Trybus E, Krol G, Obarzanowski T, Trybus W, Kopacz-Bednarska A, Obarzanowski M and Krol T: In vivo and in vitro studies on multidirectional mechanism of anti-allergic activity of budesonide. J Physiol Pharmacol 68: 907-919, 2017.
17. Kim HY, Cheon JH, Lee SH, Min JY, Back SY, Song JG, Kim DH, Lim SJ and Han HK: Ternary nanocomposite carriers based on organic clay-lipid vesicles as an effective colon-targeted drug delivery system: Preparation and in vitro/in vivo characterization. J Nanobiotechnology 18: 17, 2020.

18. Xu G, Mo L, Wu C, Shen X, Dong H, Yu L, Pan P and Pan K: The miR-15a-5p-XIST-CUL3 regulatory axis is important for sepsis-induced acute kidney injury. Ren Fail 41: 955-966, 2019.
19. Peng Y, Liu L, Wang Y, Yao J, Jin F, Tao T, Yuan H, Shi L and Lu S: Treatment with toll-like receptor 2 inhibitor ortho-vanillin alleviates lipopolysaccharide-induced acute kidney injury in mice. Exp Ther Med 18: 4829-4837, 2019.
20. Zhang W, Qi R, Li T, Zhang X, Shi Y, Xu M and Zhu T: Kidney organoids as a novel platform to evaluate lipopolysaccharide-induced oxidative stress and apoptosis in acute kidney injury. Front Med (Lausanne) 8: 766073, 2021.
21. Ying ZH, Li HM, Yu WY and Yu CH: Iridin prevented against lipopolysaccharide-induced inflammatory responses of macrophages via inactivation of PKM2-mediated glycolytic pathways. J Inflamm Res 14: 341-354, 2021.
22. Tong C, Wu H, Gu D, Li Y, Fan Y, Zeng J and Ding W: Effect of curcumin on the non-alcoholic steatohepatitis via inhibiting the M1 polarization of macrophages. Hum Exp Toxicol 40 (12_suppl): S310-S317, 2021.
23. Wang C, Yue Y, Huang S, Wang K, Yang X, Chen J, Huang J and Wu Z: M2b macrophages stimulate lymphangiogenesis to reduce myocardial fibrosis after myocardial ischaemia/reperfusion injury. Pharm Biol 60: 384-393, 2022.
24. Zhang HX, Yuan J, Li YF and Li RS: Thalidomide decreases high glucose-induced extracellular matrix protein synthesis in mesangial cells via the AMPK pathway. Exp Ther Med 17: 927-934, 2019.
25. Ponticelli C and Locatelli F: Glucocorticoids in the treatment of glomerular diseases: Pitfalls and pearls. Clin J Am Soc Nephrol 13: 815-822, 2018.
26. Nuñez FJ, Johnstone TB, Corpuz ML, Kazarian AG, Mohajer NN, Tliba O, Panettieri RA Jr, Koziol-White C, Roosan MR and Ostrom RS: Glucocorticoids rapidly activate cAMP production via $G_{\alpha s}$ to initiate non-genomic signaling that contributes to one-third of their canonical genomic effects. FASEB J 34: 2882-2895, 2020.
27. Kan M, Koziol-White C, Shumyatcher M, Johnson M, Jester W, Panettieri RA Jr and Himes BE: Airway smooth muscle-specific transcriptomic signatures of glucocorticoid exposure. Am J Respir Cell Mol Biol 61: 110-120, 2019.
28. Zhang H, Liu B, Jiang S, Wu JF, Qi CH, Mohammadtursun N, Li Q, Li L, Zhang H, Sun J and Dong JC: Baicalin ameliorates cigarette smoke-induced airway inflammation in rats by modulating HDAC2/NF-κB/PAI-1 signalling. Pulm Pharmacol Ther 70: 102061, 2021.
29. Mostafa MM, Rider CF, Shah S, Traves SL, Gordon PMK, Miller-Larsson A, Leigh R and Newton R: Glucocorticoid-driven transcriptomes in human airway epithelial cells: Commonalities, differences and functional insight from cell lines and primary cells. BMC Med Genomics 12: 29, 2019.
30. Zhang Y and Wang H: Efficacy of montelukast sodium chewable tablets combined with inhaled budesonide in treating pediatric asthma and its effect on inflammatory factors. Pharmazie 74: 694-697, 2019.
31. Chen L, Huang M and Xie N: The effect of montelukast sodium plus budesonide on the clinical efficacy, inflammation, and pulmonary function in children with cough variant asthma. Am J Transl Res 13: 6807-6816, 2021.
32. Zhang Y and Li B: Effects of montelukast sodium plus budesonide on lung function, inflammatory factors, and immune levels in elderly patients with asthma. Ir J Med Sci 189: 985-990, 2020.
33. Dong L, Zhu YH, Liu DX, Li J, Zhao PC, Zhong YP, Chen YQ, Xu W and Zhu ZQ: Intranasal application of budesonide attenuates lipopolysaccharide-induced acute lung injury by suppressing nucleotide-binding oligomerization domain-like receptor family, pyrin domain-containing 3 inflammasome activation in mice. J Immunol Res 2019: 7264383, 2019.
34. Shapouri-Moghaddam A, Mohammadian S, Vazini H, Taghadosi M, Esmaeili SA, Mardani F, Seifi B, Mohammadi A, Afshari JT and Sahebkar A: Macrophage plasticity, polarization, and function in health and disease. J Cell Physiol 233: 6425-6440, 2018.
35. Lu J, Xie L and Sun S: The inhibitor miR-21 regulates macrophage polarization in an experimental model of chronic obstructive pulmonary disease. Tob Induc Dis 19: 69, 2021.
36. Chen Z, Wu H, Shi R, Fan W, Zhang J, Su W, Wang Y and Li P: miRNAomics analysis reveals the promoting effects of cigarette smoke extract-treated Beas-2B-derived exosomes on macrophage polarization. Biochem Biophys Res Commun 572: 157-163, 2021.
37. Su JC, Zhang Y, Chen C, Zhu YN, Ye YM, Sun YK, Xiang SY, Wang Y, Liu ZB and Zhang XF: Hydrogen regulates the M1/M2 polarization of alveolar macrophages in a rat model of chronic obstructive pulmonary disease. Exp Lung Res 47: 301-310, 2021.
38. Lin YC, Lin YC, Tsai ML, Tsai YG, Kuo CH and Hung CH: IL-33 regulates M1/M2 chemokine expression via mitochondrial redox-related mitophagy in human monocytes. Chem Biol Interact 359: 109915, 2022.
39. Li Q, Lu L, Li X and Lu S: Long non-coding RNA NKILA alleviates airway inflammation in asthmatic mice by promoting M2 macrophage polarization and inhibiting the NF-κB pathway. Biochem Biophys Res Commun 571: 46-52, 2021.
40. Liu Y, Gao X, Miao Y, Wang Y, Wang H, Cheng Z, Wang X, Jing X, Jia L, Dai L, *et al*: NLRP3 regulates macrophage M2 polarization through up-regulation of IL-4 in asthma. Biochem J 475: 1995-2008, 2018.
41. Shang Y, Sun Y, Xu J, Ge X, Hu Z, Xiao J, Ning Y, Dong Y and Bai C: Exosomes from mmu_circ_0001359-modified ADSCs attenuate airway remodeling by enhancing FoxO1 signaling-mediated M2-like macrophage activation. Mol Ther Nucleic Acids 19: 951-960, 2020.
42. Han J, Pang X, Zhang Y, Peng Z, Shi X and Xing Y: Hirudin protects against kidney damage in streptozotocin-induced diabetic nephropathy rats by inhibiting inflammation via P38 MAPK/NF-κB pathway. Drug Des Devel Ther 14: 3223-3234, 2020.
43. Fan HY, Wang XK, Li X, Ji K, Du SH, Liu Y, Kong LL, Xu JC, Yang GQ, Chen DQ and Qi D: Curcumin, as a pleiotropic agent, improves doxorubicin-induced nephrotic syndrome in rats. J Ethnopharmacol 250: 112502, 2020.
44. Yu N, Yang L, Ling L, Liu Y, Yu Y, Wu Q, Gu Y and Niu J: Curcumin attenuates angiotensin II-induced podocyte injury and apoptosis by inhibiting endoplasmic reticulum stress. FEBS Open Bio 10: 1957-1966, 2020.
45. Zhang P, Fang J, Zhang J, Ding S and Gan D: Curcumin inhibited podocyte cell apoptosis and accelerated cell autophagy in diabetic nephropathy via regulating Beclin1/UVRAG/Bcl2. Diabetes Metab Syndr Obes 13: 641-652, 2020.
46. Shi L, Xiao C, Zhang Y, Xia Y, Zha H, Zhu J and Song Z: Vitamin D/vitamin D receptor/Atg16L1 axis maintains podocyte autophagy and survival in diabetic kidney disease. Ren Fail 44: 694-705, 2022.
47. Li M, Liu X and Zhang Z: Hyperglycemia exacerbates cadmium-induced glomerular nephrosis. Toxicol Ind Health 37: 555-563, 2021.
48. Wadey KS, Somos A, Cross SJ, Reolizo LM, Johnson JL and George SJ: Monitoring cellular proliferation, migration, and apoptosis associated with atherosclerosis plaques in vitro. Methods Mol Biol 2419: 133-167, 2022.
49. Liu QZ, Chen XD, Liu G and Guan GJ: Identification and isolation of kidney-derived stem cells from transgenic rats with diphtheria toxin-induced kidney damage. Exp Ther Med 12: 1651-1656, 2016.
50. Suzuki T, Eng DG, McClelland AD, Pippin JW and Shankland SJ: Cells of NG2 lineage increase in glomeruli of mice following podocyte depletion. Am J Physiol Renal Physiol 315: F1449-F1464, 2018.
51. Wei SY, Guo S, Feng B, Ning SW and Du XY: Identification of miRNA-mRNA network and immune-related gene signatures in IgA nephropathy by integrated bioinformatics analysis. BMC Nephrol 22: 392, 2021.
52. Peng W, Pei GQ, Tang Y, Tan L and Qin W: IgA1 deposition may induce NLRP3 expression and macrophage transdifferentiation of podocyte in IgA nephropathy. J Transl Med 17: 406, 2019.
53. Ji L, Chen Y, Wang H, Zhang W, He L, Wu J and Liu Y: Overexpression of Sirt6 promotes M2 macrophage transformation, alleviating renal injury in diabetic nephropathy. Int J Oncol 55: 103-115, 2019.
54. Yang H, Xie T, Li D, Du X, Wang T, Li C, Song X, Xu L, Yi F, Liang X, *et al*: Tim-3 aggravates podocyte injury in diabetic nephropathy by promoting macrophage activation via the NF-κB/TNF-α pathway. Mol Metab 23: 24-36, 2019.
55. Liao H, Li Y, Zhang X, Zhao X, Zheng D, Shen D and Li R: Protective effects of thalidomide on high-glucose-induced podocyte injury through in vitro modulation of macrophage M1/M2 differentiation. J Immunol Res 2020: 8263598, 2020.
56. Kong DH, Kim YK, Kim MR, Jang JH and Lee S: Emerging roles of vascular cell adhesion molecule-1 (VCAM-1) in immunological disorders and cancer. Int J Mol Sci 19: 1057, 2018.

57. Wagner C, Uliczka K, Bossen J, Niu X, Fink C, Thiedmann M, Knop M, Vock C, Abdelsadik A, Zissler UM, *et al*: Constitutive immune activity promotes JNK- and FoxO-dependent remodeling of Drosophila airways. Cell Rep 35: 108956, 2021.
58. Caramori G, Ruggeri P, Arpinelli F, Salvi L and Girbino G: Long-term use of inhaled glucocorticoids in patients with stable chronic obstructive pulmonary disease and risk of bone fractures: A narrative review of the literature. Int J Chron Obstruct Pulmon Dis 14: 1085-1097, 2019.
59. Almeida M and Porter RM: Sirtuins and FoxOs in osteoporosis and osteoarthritis. Bone 121: 284-292, 2019.
60. Long Z, Wu J, Xiang W, Zeng Z, Yu G and Li J: Exploring the mechanism of icariin in osteoporosis based on a network pharmacology strategy. Med Sci Monit 26: e924699, 2020.
61. Pattrapornpisut P, Avila-Casado C and Reich HN: IgA nephropathy: Core curriculum 2021. Am J Kidney Dis 78: 429-441, 2021.
62. Barbour SJ, Coppo R, Zhang H, Liu ZH, Suzuki Y, Matsuzaki K, Katafuchi R, Er L, Espino-Hernandez G, Kim SJ, *et al*: Evaluating a new international risk-prediction tool in IgA nephropathy. JAMA Intern Med 179: 942-952, 2019.